Event-triggered distributed voltage regulation by heterogeneous BESS in low-voltage distribution networks

Kang, Wenfa; Chen, Minyou; Guan, Yajuan; Wei, Baoze; Vasquez Q., Juan C.; Guerrero, Josep M.

Published in:
Applied Energy

DOI (link to publication from Publisher):
10.1016/j.apenergy.2022.118597

Publication date:
2022

Document Version
Accepted author manuscript, peer reviewed version

Event-triggered Distributed Voltage Regulation by Heterogeneous BESS in Low-Voltage Distribution Networks

Wenfa Kang[a], Minyou Chen[a], Yajuan Guan[b], Baoze Wei[b], Juan C. Vasquez Q.[b] and Josep M. Guerrero[b]

[a] *State Key Laboratory of Power Transmission Equipment & System Security and New Technology, School of Electrical Engineering, Chongqing University, Chongqing 400044, China*

[b] *Center for Research on Microgrids (CROM), AAU Energy, Aalborg University, 9220 Aalborg East, Denmark (Tel: +45 2037 8262; Fax: +45 9815 1411; e-mail: joz@et.aau.dk)*

Abstract

High penetration level of PV sources in low-voltage distribution network (LVDN) leads to the voltage fluctuation problem, which may limit the maximal PV power generation due to the security issues of distribution networks. This paper proposes a distributed voltage regulation method by sharing the power of distributed heterogeneous battery energy storage systems (BESS) properly. With the help of local voltage/power droop controller, BESS absorbs power from LVDN when nodal voltage is above the upper limit, and injects power to LVDN when nodal voltage is lower than the bottom limit. The voltage regulation burden is properly shared among BESSs not only according to the capacities but also the state of charge (SoC). Moreover, even the communication network among BESSs is time-varying, the proposed method is able to regulate nodal voltages. For an extreme scenario with communication failures, the proposed method can also guarantee the voltage regulation and power sharing locally. Furthermore, a dynamic event-triggered communication strategy is designed for BESS aiming at reducing communication burden. Four simulation cases are designed on MATLAB/Simulink to validate the effectiveness of the proposed method. The results show that the proposed method is capable of maintaining nodal voltages within the normal range, and achieves the proportional regulation and SoC balance among different BESS with reduced communications.

Keywords: Voltage regulation, Low-voltage distribution network, Battery Energy Storage System (BESS), Event-triggered control, SoC balancing

1. Introduction

Integration of photovoltaic (PV) systems in Distribution Networks (DN), brings various benefits to our society due to its environmentally friendly energy and the declining price [1, 2]. Penetration of PV resources is rapidly growing in various ways, e.g., PV station, rooftop PV, distributed PV. However, one of the major issues is the voltage fluctuation, especially in the long and radial low-voltage DN, which affects the system operation and needs to be concerned [3, 4].

Connection of PV systems turned the original passive DN into the modern active DN, since the one-way direction of power flow becomes two-way directions of power flow. Voltage rise issues occur toward the end of a distribution feeder whenever the surplus power flows from PV sources to the point of common coupling (PCC), namely, the power supply of PV sources is higher than the power demand of loads. Thus, consumers towards the end of network suffer from the voltage rise problem. PV sources may be disconnected from the network due to the protection purpose if the voltage magnitudes are out of the normal range. Over-voltage problems will in turn lead to the low harvesting efficiency of PV energy.

Different strategies have been investigated to regulate nodal voltages, including switching on/off capacitors [5] and adjusting tap positions of tap-changing transformers [6, 7], adjusting active and reactive power of distributed generators (DG) [8], curtailment of PV power [9, 10, 11] and adjustment of battery energy storage systems (BESS) power [12, 13, 14]. Usually, nodal voltage is regulated by adjusting the active/reactive power injected/absorbed into/from networks at some related nodes. The proper power injection/absorption at those nodes is obtained from optimizing power flow model with voltage constraints or designing local power/voltage droop controller. Thus, based on the method obtaining proper power injection/absorption, voltage regulation strategies can be classified into two categories, i.e., optimization based strategies [15, 16, 17, 18, 19, 20, 21, 22] and feedback controller based strategies [10, 23, 24, 25, 26, 27, 28].

By solving the optimal power flow problem, optimization based voltage regulation strategies can obtain the power references for the adjustable units, such as DG, BESS, PV systems, and even capacitors and on-load tap changers (OLTC) [22, 29, 30]. Reference [15] proposed a scenario based Volt/var control model to schedule the reactive power of DG in order to drive voltage into the normal range. In [16], a mixed-integer second-order cone programming (MISOCP) model was formulated to

*Corresponding author: Wenfa Kang(kwf.ac@outlook.com)
**Principal corresponding author:Minyou Chen(minyouchen@cqu.edu.cn)

regulate voltage of distribution network by adjusting reactive and active power of DG. While in [17], a randomized algorithm is proposed to achieve voltage regulation in distribution networks via coordinated regulation of the active and reactive power of DGs. By partitioning distribution network, a double-layer voltage control strategy is proposed in reference [18] to optimize the active and reactive power outputs of PV units. By control the active and reactive transmission of soft open point, a combined decentralized and local voltage control strategy is provided in [19] to smoothen the frequent voltage fluctuations. Focusing on voltage regulation problem of wind farms, an online optimization method is proposed in [20] to adjust reactive power outputs of wind turbines and static synchronous compensators coordinately. In [22], a distributed coordinated voltage control scheme is designed to control reactive power of static synchronous compensators, DG and OLTC to drive nodal voltages to be close to the nominal value in the distribution network. Two-timescale voltage control model is proposed in [31] to regulate the reactive power of inverters and to control shunt capacitors, where the outputs of inverters are adjusted in fast timescale (in minutes) and the states (on or off) of shunt capacitors are adjusted in slow time-scale (in hours).

Nodal voltages are always theoretically restrained in the normal range since the reference of nodal power is optimized by solving the optimal power flow problem with voltage constraints. It is difficult and time-consuming to solve an optimal power flow management problem because of the nonlinear and non-convex property. For that reason, the DistFlow model or relaxation method is often adopted to build the optimal power flow model [15, 17, 20, 32, 30]. Normally, these approaches which are optimizing reactive power in distribution network need to be aware of the knowledge of distribution networks so that voltage is regulated by adjusting reactive power. Besides, voltage rising problem is dominated by active power injection in low voltage distribution networks with high resistance-reactance ratio. Therefore, voltage regulation method by optimizing reactive power seems not very effective to regulate nodal voltages in low-voltage DN. Moreover, optimized reactive/active power references are sent to DG/PVs only after solving the relevant voltage regulation optimization problems. Thus, voltage regulation speed mainly depends on the convergence speed of optimization algorithms.

On the other hand, methods with stable voltage feedback controller are simple and have high scalability to the implementation, since only voltage is used in the local voltage controller [10, 16, 23, 25, 26, 28, 33, 34]. Due to the declining cost of BESS, the household BESS or the combination of PV and BESS is installed widely in communities and consumers' side [25, 28]. BESS can absorb the surplus power from the network such that voltage-rise problem can be mitigated, meanwhile BESS injects power to the grid such that the voltage-dip problem can also be solved. BESS maximizes the usage of PV energy since no power curtailment of PV occurs. Energy storage unit installed at the consumer' side was adopted to mitigate nodal voltage rise caused by PV power, where a leader-following consensus algorithm was used to coordinate the power of energy storage unit [34]. However, the energy capacity constraint of storage unit was not considered. While in [23], a coordinated control strategy, composed of distributed ESS power control and localized SoC control, was designed to drive nodal voltages into the normal range. Mehdi *et.al* proposed a distributed control strategy for BESS aiming at achieving voltage regulation of low-voltage DN, where two consensus algorithms were designed for sharing regulation burden according to BESS capacities and SoC values, respectively. Furthermore, consensus algorithm was used to adjust the power of plug-in electric vehicles such that nodal voltages can be regulated cooperatively. When the capacities of electric vehicles are not available, voltage regulation was achieved by curtailing PV power. In order to achieve proportional power curtailment of PV, another similar consensus algorithm was used [10]. Similarly, reactive power sharing strategy of single-phase PV inverters was proposed to drive system voltage into the normal range in low-voltage DN [26]. In [28], a distributed voltage regulation method robust to the bounded communication delay was investigated. In [33], measurement data from distribution phasor measurement units was adopted to calculate the nodal voltage-power sensitivity, according to which voltage regulation was achieved locally.

In the aforementioned references [10, 23, 25, 26, 28, 33, 34], local voltage/power droop controller is the key to achieve voltage regulation. And consensus algorithms are adopted to share the voltage regulation burden among BESS and PV sources, so that each BESS or PV participates to voltage regulation cooperatively. However, methods in these references need continuous and perfect communications among agents which is communication costly. And the parameter differences of BESS are not fully considered in these references. In operations, communications may be imperfect owing to data congestions or natural destructions. In a DN, BESS with different capacities and working efficiencies may be installed at the various nodes. This paper brings a high-efficient method to control/manage the distributed and heterogenous BESS to fulfill the target of voltage regulation. To cover these gaps, a distributed even-triggered voltage regulation method by sharing BESS power considering both the time-varying communication networks and communication link failures is proposed. Moreover, the parameter differences of BESS, such as capacities and charging/discharging efficiencies, are considered in this paper. To conclude, the contribution of this paper is represented as

- Compared with the centralized methods in voltage regulation, a novel distributed optimal strategy with high scalability, free of single-point failure, for voltage regulation in LVDN with high penetrated PV systems is proposed using heterogeneous BESS, which not only maintains the bus voltage within the normal range but also guarantees the proper power sharing.
- An optimal control gain is designed for SoC balancing and proportional power sharing of BESS with different parameters, even if the communication network among BESS is time-varying.
- Compared with the aforementioned distributed approaches

in [19, 22, 31] and in [10, 20, 25, 26, 28, 35], a dynamic event-triggered communication strategy using self-states for BESS power and energy sharing is designed in order to reduce the communication burden.

- The proposed method is also robust to the communication link failures. The nodal voltage regulation, energy and power sharing can be achieved locally, even if the communication link failures occur.

This paper is organized as follows. In Section 2, the model of voltage regulation and power sharing are formulated. Distributed event-triggered power control strategy for heterogeneous BESS over constant communication network, time-varying communication networks and communication link failures are introduced in Section 3. Simulation experiments and the results analysis are presented in Section 4. Section 5 concludes the paper.

2. Problem Formulation

2.1. Voltage Limits Violation Issues of Distribution Networks

Fig. 1 shows a distribution network with n nodes, where node voltages are decided by power line flows $P_{Line,i}$ and $Q_{Line,i}$, power line resistance $L_{R,i}$ and reactance $L_{X,i}$ and neighbors' voltage amplitude V_{i-1} [36, 35], which are show in equation (1).

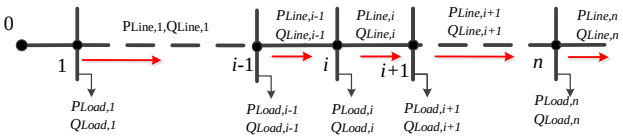

Figure 1: Low voltage distribution network with n nodes.

$$\begin{cases} P_{\text{Line},i} = P_{\text{Line},i-1} - L_{R,i-1}\dfrac{P^2_{\text{Line},i-1} + Q^2_{\text{Line},i-1}}{V^2_{i-1}} - P_{\text{Load},i} \\ Q_{\text{Line},i} = Q_{\text{Line},i-1} - L_{X,i-1}\dfrac{P^2_{\text{Line},i-1} + Q^2_{\text{Line},i-1}}{V^2_{i-1}} - Q_{\text{Load},i} \\ V^2_i = V^2_{i-1} - 2\left(L_{R,i-1}P_{\text{Line},i-1} + L_{X,i-1}Q_{\text{Line},i-1}\right) \\ \qquad + \left(L^2_{R,i-1} + L^2_{X,i-1}\right)\dfrac{P^2_{\text{Line},i-1} + Q^2_{\text{Line},i-1}}{V^2_{i-1}} \end{cases} \tag{1}$$

In term with equation (1), one can see voltage V_i will be larger than V_{i-1} when power $P_{Line,i-1}$ and $Q_{Line,i-1}$ are negative (reverse power flow) caused by PV generation. Meanwhile, in low-voltage distribution network with high penetration of PV, the ratio of $L_{R,i}/L_{X,i}$ is relative large, thus, voltage rise issues are mainly caused by PV active power injection.

BESSs are widely adopted to solve voltage regulation problems, since BESS can absorb or inject power from/to distribution network. A low-voltage distribution network with BESS and PV sources is shown in Fig.2. When power supply of PV is higher than power demand of loads, BESS can absorb surplus

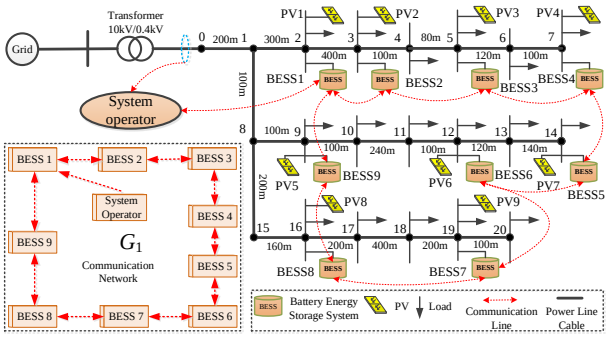

Figure 2: Distribution network with a group of heterogeneous BESS, PV sources and loads.

power from LVDN in order to keep power balance. On the contrary, BESS will provide power to LVDN when load demand is higher than power supply of PV. Apart from keeping power balance, BESS can be used to mitigate voltage rise/voltage dip issues caused by PV and load demand. To conclude, BESS are available to work in two modes, voltage regulation mode and power sharing mode.

- To drive voltage magnitude into the normal range, when $V_i(t) > V_{max}$, BESS absorb power from LVDN.
- To drive voltage magnitude into the normal range, when $V_i(t) < V_{min}$, BESS provide power to LVDN.
- When $V_{min} \leq V_i(t) \leq V_{max}$, BESS share voltage regulation burden according to its capacity and SoC.

2.2. BESS Model and Control

Traditionally, battery energy storage systems (BESS) are composed of battery packages, DC/AC converter, LCL filter, and converter controller. The control model of BESS with voltage regulation is shown in Fig. 3. In voltage regulation mode, BESS calculates power set-point according to the controller (4), while in power sharing mode, BESS calculates set-point according to the controller (6). The setpoint of BESS power is then sent to the primary control loops. Moreover, the basic

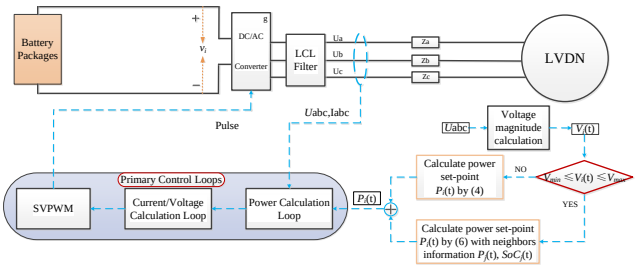

Figure 3: The control model of BESS.

method to calculate the state of charge (SoC) of battery is based on coulomb counting [37, 38], which is

$$\dot{SoC}_i(t) = -\frac{\eta_i}{c_i} I_i(t), \tag{2}$$

where η_i is the Coulombic efficiency. Normally, the output voltage of BESS is close to the reference point [39], thus, equation (2) can be formulated as

$$\begin{cases} S\dot{o}C_i(t) = -\dfrac{\eta_i}{c_i \cdot v_i} P_i(t), \\ P_i(t) = v_i \cdot I_i(t), \quad i = 1, \cdots, N, \end{cases} \tag{3}$$

where $c_i(Ah)$, $v_i(V)$, η_i and $P_i(t)(kW)$ are BESS capacity, working voltage, efficiency and power output of BESS.

2.3. PV Model and Control

The model of PV system is shown in Fig. 4. PV model is composed of maximal power point tracking (MPPT) control, DC voltage control and DC/AC controller. By controlling DC voltage U_0, DC power is converted into AC power. PV power output is dominated by solar irradiation. In simulation, one can change solar irradiation signal to change PV power output. In the control process, PV works in MPPT mode, that is, the power outputs of PV depend on solar irradiation.

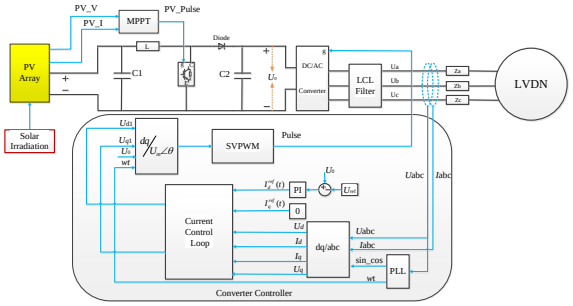

Figure 4: The control model of PV system.

2.4. Voltage Regulation Mode

When voltage violation problems occur, BESS works in voltage regulation mode. When voltage limits violations occur, the power output of BESS i is adjusted as following rules

$$\begin{cases} \dot{P}_i(t) = \alpha_1 \left(V_{max} - V_i(t)\right), & V_i(t) > V_{max}, \\ \dot{P}_i(t) = \alpha_2 \left(V_{min} - V_i(t)\right), & V_i(t) < V_{min}, \\ \dot{P}_i(t) = U_i(t), & V_{min} \le V_i(t) \le V_{max}. \end{cases} \tag{4}$$

where V_{min}, V_{max} and $U_i(t)$ are the minimal and maximal limits of node voltages, control input of BESS i, respectively. Positive α_1 and α_2 are coefficients of droop control. When nodal voltage of BESS i is larger than the upper limit, BESS i absorbs the surplus power. On the contrary, BESS i injects power into the DN when nodal voltage is below the bottom limit. The third term of equation (4) shows that when nodal voltage is within the normal range, the power outputs of BESS are adjusted by $U_i(t)$ which derives from the distributed control method to be designed later.

2.5. Power Sharing Mode

In order to enhance the work efficiency of BESS, BESS with large capacity should share more power than BESS with small capacity. Besides, during the operation, to avoid sudden shutdown of some BESS caused by low/high SoC, system power should be shared accordingly to the SoC and capacity. A BESS with high SoC and large capacity will provide more power when PV power is in a shortage, and a BESS with low SoC and small capacity will provide less power. Therefore, following objectives and constraints should be satisfied during the power sharing mode

$$\begin{cases} \lim\limits_{t\to\infty} \left|SoC_i(t) - SoC_j(t)\right| = 0, \ i, j = 1, \cdots, n, \\ \lim\limits_{t\to\infty} \left|\dfrac{P_i(t)}{C_i} - \dfrac{P_j(t)}{C_j}\right| = 0, \ i, j = 1, \cdots, n, \\ P_i^{min} \le P_i(t) \le P_i^{max}, \\ SoC_i^{min} \le SoC_i(t) \le SoC_i^{max}, \\ C = \left[\dfrac{c_1 v_1}{\eta_1}, \cdots, \dfrac{c_i v_i}{\eta_i}, \cdots, \dfrac{c_n v_n}{\eta_n}\right], i = 1, \cdots, n, \end{cases} \tag{5}$$

where P_i^{min} and P_i^{max} are the minimal and maximal power outputs of BESS, meanwhile SoC_i^{min} and SoC_i^{max} are the minimal and maximal SoC values of BESS. C_i is the i_{th} entry of the vector C, which is defined as $c_i v_i/\eta_i$. According to the definition of parameter C, if proportions of all BESS become converged, BESS with larger capacity c_i will provide more power meanwhile BESS with small capacity provide less power.

The flowchart of operation and process to solve the voltage regulation and power sharing is shown in Fig.5. Each BESS measures the nodal voltage magnitude and its power output. Then BESS chooses different working modes according to the nodal voltage magnitudes. If voltage is varying in the normal range, i.e., $V_{min} \le V_i(t) \le V_{max}$, BESS adjusts its power to achieve proportional power sharing and SoC sharing, using controller (5). If voltage is not in the normal range ($V_i(t) \le V_{min}$ or $V_{max} \le V_i(t)$), BESS adjusts its power outputs according to controller (4).

3. Distributed Event-triggered Control Methods for Heterogeneous BESS

3.1. Distributed Controller Design over Time-invariant Balanced Graph

As illustrated in Fig.2, the communication network of n BESS can be regarded as an unbalanced graph $G_1(N, E)$, where BESS is regarded as a node in communication network, and each edge is the communication link between two BESSs. Denote $\mathcal{A} = [a_{ij}]_{n\times n}$ as the adjacent matrix of a graph where $a_{ij} = a_{ji} = 1$ if and only if there is a communication link between node i and node j. Otherwise $a_{ij} = a_{ji} = 0$. While the Laplacian matrix $L = [L_{ij}]_{n\times n}$ is defined as $L = D - \mathcal{A}$, where diagonal matrix D is the out-degree matrix of graph $G_1(N, E)$.

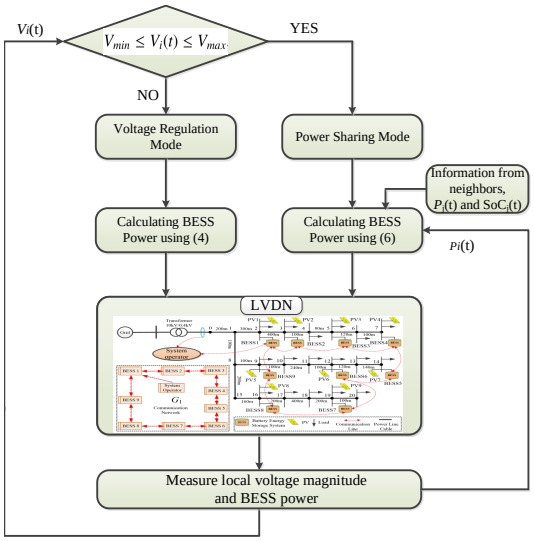

Figure 5: Flowchart of voltage regulation and power sharing process.

In order to share power among BESS according to their capacities and SoC, control method is designed as

$$U_i(t) = \underbrace{\beta_1 \sum_{j\in n_i} L_{ij} SoC_j(t)}_{\texttt{Term 1}} + \underbrace{C_0\beta_2 \sum_{j\in n_i} C_i^{-1} L_{ij} P_j(t)}_{\texttt{Term 2}}, \tag{6}$$

where β_1 and β_2 are the feedback control gains to be designed. $C^{-1} = diag\left[C_1^{-1}, \cdots, C_n^{-1}\right]$, and C_0 is the minimal entry of vector C. n_i is the set of neighbors of BESS i. $L = [L_{ij}]_{n\times n}$ is the Laplacian matrix of a balanced graph G_1. In (6), `Term 1` is designed to ensure SoC synchronized, and `Term 2` is used to guarantee proportional power sharing. Feedback control gains β_1, β_2 are designed to guarantee the stability of control laws (6).

In controller (6), information of $SoC_i(t)$ and $P_i(t)$ are transmitted over the communication network. In order to reduce communication burden, event-triggered information delivery strategy and controller are designed by (7) and (9),

$$\begin{cases} f_i\left(SoC_i(t), P_i(t)\right) \\ = \left(\left(SoC_i(t) - SoC_i(t_k^i)\right)^2 + \left(P_i(t) - P_i(t_k^i)\right)^2\right) \\ - \dfrac{\delta^2}{(1+t)^2}\left(SoC_i(t_k^i)^2 + P_i(t_k^i)^2\right), \end{cases} \tag{7}$$

where positive parameter δ needs to be designed to maintain system stability. Meanwhile, the event-triggered time instant is defined as

$$t_{k+1}^i = \texttt{inf}\left\{t > t_k^i \mid f_i(t) > 0\right\}. \tag{8}$$

In equation $t_{k+1}^i = \texttt{inf}\left\{t > t_k^i | f_i(t) > 0\right\}$, t_k^i is the k^{th} triggered time instant of BESS i, and t_{k+1}^i is the $k+1^{th}$ possible triggered time instant of BESS i. Coherently, for the i^{th} BESS, the distributed controller with event-triggered information transmission strategy (7) can be designed as

$$U_i(t) = \underbrace{\beta_1 \sum_{j\in n_i} L_{ij} SoC_j(t_k^j)}_{\texttt{Term 1}} + \underbrace{C_0\beta_2 \sum_{j\in n_i} C_i^{-1} L_{ij} P_j(t_k^j)}_{\texttt{Term 2}}, \tag{9}$$

where $i = 1, \cdots, n$.

Next is to find reasonable feedback control gain β_1, β_2 and parameter δ to ensure that controller (9) is stable.

Theorem 1: For a connected and balanced graph, the proposed objectives (5) can be fulfilled if feedback control gain $K = [\beta_1, \beta_2]$ and parameter δ of controller (9) satisfy the following condition

$$\begin{cases} K = aB^T P, \\ \delta^2 < \dfrac{\lambda_2^2}{\lambda_2^2 + \lambda_n^2}, \end{cases} \tag{10}$$

where positive matrix $P > 0$ is a solution of following equality

$$PA + A^T P - aPBB^T P + bQ \le 0 \tag{11}$$

where $0 < a \le \frac{2J_2}{\lambda_n}$, $b \ge 2\lambda_n$, $A = [0, a_{12}; 0, 0]$, a_{12}=1e-3, $B = [0, 1]^T$, and Q is a positive constant matrix. λ_2, J_2 are the smallest nonzero eigenvalues of matrix L and $W = C_0 L C^{-1} L$ separatively, λ_n is the largest eigenvalue of matrix L.

Remark 1: Theorem 1 provides a guideline to choose the control gain $K = [\beta_1, \beta_2]$ and δ which guarantee the controller (9) stable. In theorem 1, system matrix A is designed according to the model of SoC and power outputs of BESS. The matrix Q is a given positive matrix related to the control performance, described by expression (17). While the weighted control matrix $W = C_0 L C^{-1} L$ is used to achieve the proportional power sharing of BESS. For a system with given parameters, Laplacian matrix L and weighted matrix W are all known. So feedback control gain K can be obtained by choosing proper Q, a and b and solving inequality (11). With the chosen δ and obtained control gain K, controller (9) is designed. During power sharing model, the proposed event-triggered control method (9), containing SoC synchronization term and proportional convergence term, can also ensure the mentioned objectives. Besides, communication times among BESS can be reduced owing to the event-triggered information transmission strategy. From (7), it can be seen that the event-function is only decided by its states, which simplifies the design of event-triggered strategy.

Proof: Combine (3) and (6), the state model of BESS with controller (9) is obtained as

$$\dot{X}(t) = \left(I_n \otimes A - C_0 C^{-1} L \otimes (BK)\right)(X(t) + e(t)). \tag{12}$$

where $e_i(t) = X_i(t_k^i) - X_i(t)$, and $e(t) = [e_1(t_k^1), \cdots, e_M(t_k^n)]_{2n\times 1}^T$ is a state error vector, and state variable $X_i(t)$ is $[SoC_i(t), P_i(t)/C_i]^T$. Choose Lyapunov function candidate as

$$V(t) = \frac{1}{2} X^T(t)(L \otimes P)X(t). \tag{13}$$

And the time derivative of $V(t)$ along the trajectory of system

(13) is

$$\begin{aligned}\dot{V}(t) &= X^T(t)\Big(L\otimes\bar{A} - W\otimes\bar{B}\Big)X(t)\\ &+ X^T(t)\Big(L\otimes\bar{A} - W\otimes\mu\bar{B}\Big)e(t)\\ &= \xi^T(t)\left(\nu^T L\nu\otimes\bar{A} - \nu^T W\nu\otimes\bar{B}\right)\xi(t)\\ &+ \xi^T(t)\left(\nu^T L\nu\otimes\bar{A} - \nu^T W\nu\otimes\bar{B}\right)\tilde{e}(t)\\ &\le \xi^T(t)\left(\lambda\otimes\bar{A} - J\otimes\bar{B}\right)\xi(t)\\ &+ \xi^T(t)\left(\lambda\otimes\bar{A} - J\otimes\bar{B}\right)\tilde{e}(t)\\ &= \sum_{i=1}^{n}\xi_i^T(t)\left(\lambda_i\bar{A} - J_i\bar{B}\right)\xi_i(t)\\ &+ \sum_{i=1}^{n}\xi_i^T(t)\left(\lambda_i\bar{A} - J_i\bar{B}\right)\tilde{e}_i(t),\end{aligned} \tag{14}$$

where $\bar{A} = \frac{A^TP+PA}{2}$, $\bar{B} = PBB^TP$, $W = C_0LC^{-1}L$, and ν is the orthogonal matrix associated with matrix W, and $\xi(t) = (\nu^T\otimes I_2)X(t)$, $\tilde{e}(t) = (\nu^T\otimes I_2)e(t)$. Using inequality (11), it derives

$$\begin{aligned}\dot{V}(t) \le& -\sum_{i=1}^{n}\lambda_i^2\xi_i^T(t)Q\xi_i(t) + \sum_{i=1}^{n}\lambda_i^2\xi_i^T(t)Q\tilde{e}_i(t)\\ \le& -\lambda_2^2\sum_{i=1}^{n}\xi_i^T(t)Q\xi_i(t) + \lambda_n^2\sum_{i=1}^{M}\xi_i^T(t)Q\tilde{e}_i(t)\\ \le& \|Q\|\left(-\lambda_2^2\|\xi_i(t)\|^2 + \lambda_n^2\|\xi_i(t)\|\cdot\|\tilde{e}_i(t)\|\right).\end{aligned} \tag{15}$$

Noting equality $\|\tilde{e}(t)\|^2 = \|e(t)\|^2$, $\|\xi(t)\|^2 = \|X(t)\|^2$, and inequality $x^T\cdot y \le \|x\|\cdot\|y\|$ for any vector $x,\ y\ \in R^n$, it derives

$$\dot{V}(t) \le \|Q\|\left(-\lambda_2^2\|X(t)\|^2 + \lambda_n^2\|X(t)\|\cdot\|e(t)\|\right) \tag{16}$$

Using inequality $\|e(t)\| \le \frac{\delta}{(1+t)^2}\|e(t)+X(t)\|$ or $\|e(t)\| \le \frac{\delta}{(1+t)^2-\delta}\|X(t)\|$, following inequality is obtained

$$\dot{V}(t) \le \|Q\|\left(-\lambda_2^2 + \frac{\delta\lambda_n^2}{(1+t)^2-\delta}\right)\|X(t)\|^2. \tag{17}$$

Thus the range of parameter δ for a stabilized controller (6) can be obtained as

$$0 < \delta < \frac{\lambda_2^2}{\lambda_2^2+\lambda_n^2}. \tag{18}$$

The proof is completed.

Theorem 2: The proposed strategy (9) excludes Zeno behavior.

Proof: The time derivative of $\|e_i(t)\|$ over the interval $\left[t_k^i, t_{k+1}^i\right)$ is

$$\begin{aligned}\frac{d\|e_i(t)\|}{dt} &= \frac{e_i(t)^T\dot{e}_i(t)}{\|e_i(t)\|} \le \left\|\frac{de_i(t)}{dt}\right\| = \left\|-\dot{X}_i(t)\right\|\\ &= \left\|-AX_i(t) + B\sum_{j=1}^{M}W_{ij}X_j(t_k^i)\right\|\\ &= \left\|-A(X_i(t_k^i) - X_i(t)) + AX_i(t_k^i) + B\sum_{j=1}^{n}W_{ij}KX_j(t_k^i)\right\|\\ &\le \left\|-A(X_i(t_k^i) - X_i(t))\right\| + \left\|AX_i(t_k^i) + B\sum_{j=1}^{n}W_{ij}KX_j(t_k^i)\right\|.\end{aligned} \tag{19}$$

Choose the maximal value of $\left\|AX_i(t_k^i) + B\sum_{j=1}^{n}W_{ij}KX_j(t_k^i)\right\|$ as θ, it derives

$$\begin{aligned}\frac{d\|e_i(t)\|}{dt} &\le \|A\|\left\|(X_i(t_k^i) - X_i(t))\right\| + \theta\\ &= \|A\|\,\|e_i(t)\| + \theta.\end{aligned} \tag{20}$$

Thus, it derives

$$\|e_i(t)\| \le \frac{\theta}{\|A\|}\left(e^{\|A\|(t-t_k^i)} - 1\right), \tag{21}$$

Then, it follows that

$$0 < \left\|e_i\left(t_{k+1}^i\right)\right\| \le \frac{\theta}{\|A\|}\left(e^{\|A\|(t_{k+1}^i - t_k^i)} - 1\right). \tag{22}$$

Finally, the inequality $t_{k+1}^i - t_k^i \ge \frac{1}{\|A\|}\ln\left(\frac{\|A\|\|e_i(t_{k+1}^i)\|}{\theta} + 1\right) > 0$ is deduced. Therefore, the time interval between two consecutive event-triggered instants is strictly larger than zero. The proof is completed.

3.2. Distributed Controller Design over Time-varying Graphs

Successful information delivery between two nodes can be hold back, due to congestion in communication networks or break-down of links therein. When these phenomena occur, the communication graphs among nodes are time-varying. This section extends the proposed strategy (9) into an application with time-varying communication networks. For example, as shown in Fig. 6, communication link between node 2 and node 3 breaks down at $t = t_1$. At $t = t_2$, communication link between node 1 and node 2 breaks down. At $t = t_3$, communication link between node 1 and node 4 as well as link between node 4 and node 3 break down. The communication graphs are changing from $G_1 \to G_2 \to G_3$ and the information is not delivered successfully at those time instants $t_1,\ t_2,\ t_3$ ($t_1 < t_2 < t_3$). Assume that the time-varying communication networks are a set of jointly connected time-varying graphs, which guarantees that the information of one node can be shared by other nodes eventually. Following theorem 3 is provided.

Theorem 3: For a set of time-varying communication networks, which are jointly connected balanced graphs, the proposed objectives (5) can also be achieved if feedback control

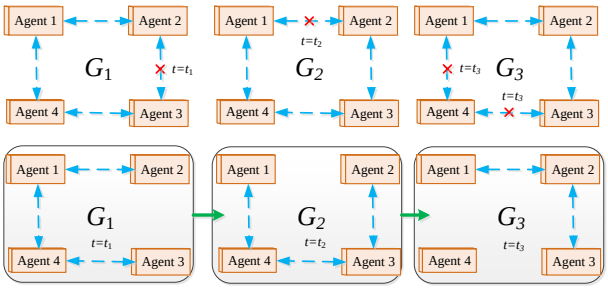

Figure 6: Time-invariant communication network changes into a set of time-varying communication networks when links between nodes break down.

gain $\kappa = [\beta_1, \beta_2]$ and parameter δ of controller (9) satisfy the following condition,

$$\begin{cases} \kappa = aB^T P, \\ \delta < \dfrac{\lambda_2(t)^2}{\lambda_2(t)^2 + \lambda_n(t)^2}, \end{cases} \tag{23}$$

where positive matrix $P > 0$ is a solution of following equality,

$$PA + A^T P - aPBB^T P + bQ \leq 0 \tag{24}$$

where $0 < a \leq \frac{2J_2(t)}{\lambda_n(t)}$, $b \geq 2\lambda_n(t)$. $\lambda_2(t)$ and $J_2(t)$ are the smallest nonzero eigenvalues of a set of time-varying matrixes $L(t)$ and $W(t)$ separatively, and $\lambda_n(t)$ is the largest eigenvalue of a set of time-varying matrixes $L(t)$.

Proof: The proof is omitted since it is similar with proofs of theorem 1 and 2.

Remark 2: For a set of balanced time-varying communication networks, feedback control gain (23) of controller (9) guarantees convergence and synchronization of BESS without Zeno behavior. The proof is similar with that of theorem 1. Since, for a given positive matrix Q, if the eigenvalues are set as $\lambda_2(t) = \mathtt{min}\{\lambda_2(t_{v1}), \cdots, \lambda_2(t_{vi}), \cdots\}$ and $\lambda_n(t) = \mathtt{max}\{\lambda_n(t_{v1}), \cdots, \lambda_n(t_{vi}), \cdots\}$, where t_{vi}, $vi = 0, \cdots, t, \cdots$, is the set of time-instants when the communication network changes, the proposed controller (23) is also stable. With the predefined eigenvalues $\lambda_2(t)$ and $\lambda_n(t)$, the stability and convergence can also be ensured. Meanwhile, the symmetry property of matrix $W(t)$, derived from the balanced communication networks, guarantees the power invariant performance of BESS, which further maintains the entire BESS power invariant during the control process. For a properly designed feedback control gain κ and δ, power sharing and SoC synchronization objectives can be achieved, even if the link between two nodes is broken down caused by data congestion or the temporary malfunction of links. It is worth noting that the events of network changing is prior to the events of event-triggered information transmission, since communication network is enforced to change due to the unexpected events, like links malfunction or data congestion. If the communication network changes, the states of BESS are immediately transmitted over the networks.

Corollary: Assume that the original connected graph G is divided into m subgraphs $G_{sub,k}$, $(k = 1, \cdots, m)$, which are all strongly connected and balanced, caused by link failures. Using the proposed controller (23), proportional power sharing and SoC balancing of BESS will be achieved locally, i.e., $\frac{P_{1,k}(t)}{C_{1,k}} = , \cdots, = \frac{P_{i,k}(t)}{C_{i,k}}$, $SoC_{1,k}(t) =, \cdots, = SoC_{i,k}(t)$, $(i = 1, \cdots, n_i,\ k = 1, \cdots, m)$, when t goes to ∞. n_i is the number of BESS in each subgraph.

Remark 3: The corollary represents an extreme condition that the original communication network is divided into several subgraphs permanently. Under the circumstance, power proportions and SoC values of BESS in each subgraph still converge to the same value, respectively. However, the global convergence fails to converge because no information sharing among different subgraphs. For a set of balanced time-varying communication networks, only if the graphs are jointly connected, global convergence can be eventually fulfilled since information sharing between two consecutive graphs always occurs.

Discussion: In order design control gain $K = [\beta_1, \beta_2]$ and the event-triggered parameter δ, theorem 1 is proposed. Theorem 1 is used to find stable control gain K and δ so that controller (9) is able to achieve the balance of the SoC and proportions of BESS, namely control objective (5). Theorem 2 is to explain that the proposed event-triggered control strategy (9) excludes the Zeno behavior, namely, the time interval between any two consecutive triggered instants is larger than zero. In other words, the control strategy (9) needs finite triggered events to convergence. Theorem 3 is an extension of theorem 1. For any balanced graphs, theorem 1 provides the guideline to choose control gain K and δ. While theorem 3 provides the guideline to choose the conservative control gain K and δ in order to guarantee the convergence of SoC and proportions of BESS even if the communication network is time-varying or switching. From the proof of theorem 1, one can know that the eigenvalues of Laplacian matrix $L(t)$ and $W = C_0 L(t) C^{-1} L(t)$ have significant impact on the convergence of the controller (9). Thus, for the condition that the communication network is time-varying, one can choose a conservative control gain K and δ to maintain convergence and stability. The performance of the proposed controller (9) is validated by numerical analysis in section 3.3. For theorem 3, section 4.3 and 4.4 show the effectiveness of the proposed controller even if the communication network is time-varying.

This approach is proposed to achieve voltage regulation and power sharing in LVDN with high-penetrated PV and distributed BESS. In order to further enhance the performance of nodal voltages, the design of optimal voltage regulator, which can accommodate power flow constraints and voltage uncertainty, is an interesting topic. Besides, the design of power sharing controller (9) with event-triggered communication strategy is based on the linearized, time-invariant model and certain model of BESS. For these situations with time-varying, uncertain and nonlinear model of BESS, further investigation of the proposed controller (9) is required. Moreover, the performance of the proposed controller needs to be further studied when communication links are threatened by cyber attacks. These concerns will be the future research motivations.

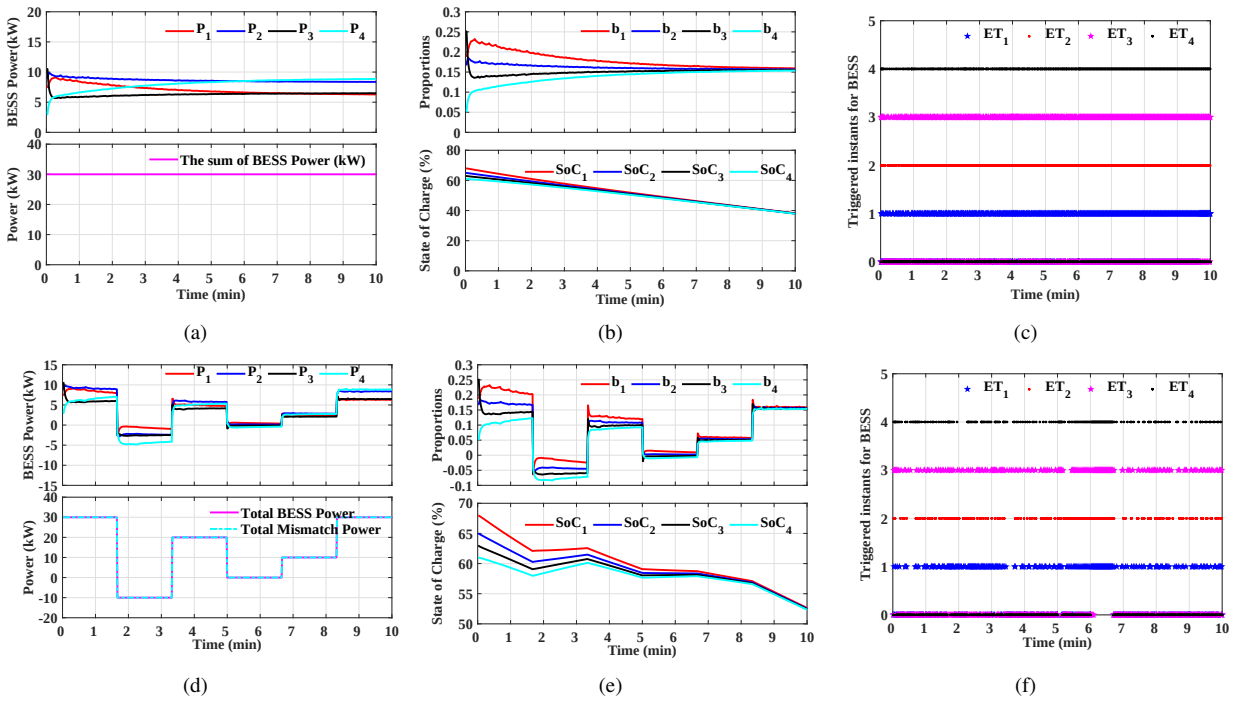

Figure 7: The states of BESS with $a = 0.1$, $b = 120$, $Q = [98e3, 1/120]$ and $\kappa = [-98.9949, 0.4459]$. (a) power outputs of BESS; (b)proportions and SoC values of BESS. (c) the triggered events of various BESS with $\sigma = 0.1$; (d) power outputs of BESS; (e) proportions and SoC values of BESS. (f) the triggered events of various BESS with $\sigma = 0.1$.

3.3. Numerical Analysis

This section investigates the convergence of the proposed power and energy sharing control methods presented in (10) and (23). Assume that there are four BESSs with different parameters installed in a low-voltage DN. Initial values of SoC are 68%, 65%, 63% and 61%, respectively. Capacities of BESS are 158(Ah), 225(Ah), 186(Ah), 252(Ah) and output voltages of BESS are 220, 216, 218, 215(V). Efficiencies of BESS are 0.88, 0.91, 0.97 and 0.94. Initial values of BESS power are 7.5, 9.0, 10.5 and 3.0 (kW). The results obtained from the time-varying communication networks (illustrated by Fig.6) are shown in Fig.7.

From Fig.7(a) and (b), it can be seen that BESS provide power according to capacities C_i, since after using the control method, proportions of BESS power gradually converge. Moreover, SoC values of BESS also converge to the same value. During the control, the sum power of BESS remains unchanged, which can be seen in Fig. 7(a). From Fig. 7(a) and parameters of different BESS, it can be seen that BESS 1 with the smallest capacity and high SoC value at the initial time provides the smallest power after convergence. While BESS 4 with the largest capacity and low SoC value at the initial time provides the largest power when SoC and proportions are converged. Therefore, according to controller (9), during the power sharing mode, BESS adjusts its power not only depends on SoC value but also its capacity. In this way, in a low-voltage DN, the voltage regulation burden will be shared more by BESS with large capacity.

Besides, it can be observed that even if the communication network among BESS is time-varying, the convergence of proportions and SoC can be achieved. Fig. 7(c) shows the triggered events of various BESS in which zero shows un-triggered events and positive values show the triggered events. These un-triggered events show that information transmission does not occur, that is, at those instants BESS does not send it states to neighbors. BESS sends its states at these triggered instants. During a control process, the more un-triggered events means the less communications among BESS. However, it should be noted that the event-triggered function $f_i\left(SoC_i(t), P_i(t)\right)$ also depends on control period/time duration t. As the control goes on, the last term of event-triggered function $f_i\left(SoC_i(t), P_i(t)\right)$ decreases, which may lead to more communications among BESS. Moreover, the variation of BESS states is also affected by voltage fluctuation. If states of BESS satisfy the triggered function, BESS will send its states to neighbors. Therefore, communication times among BESS also depend on the severity of voltage fluctuation. In practice, one can set a threshold or iteration stop criterion for states variables, namely, when the deviation of state variables is within the threshold, the control process stops and the event-triggered function is reset. When the control process stops, no communication will occur.

It can be concluded that communications among BESS are reduced since only the triggered information is delivered. Tab.1 shows the impacts of parameter δ on average communication times (C.T.), from which it can be observed that without event-triggered information delivery strategy (7) and (8), the number of communication attempts is equal to the sampling times (600). Meanwhile communication times reduce by a large margin when the strategies (7) and (8) are adopted. And, with the increasing of δ, the average communication times of each a-

gent decrease. Even when $\delta = 0.02$, more than sixty percent of communication times reduced. However, a proper parameter δ should be chosen carefully in order to balance the reduction of communication times and system performance.

Table 1: Impacts of δ to Communication Times

Parameter	$\delta = 0.1$	$\delta = 0.08$	$\delta = 0.05$	$\delta = 0.02$
C.T.	211	223	245	273

Fig.7 (d), (e) and (f) are the results which are used to show that BESS can smoothen the power fluctuation in a LVDN. Fig.7 (d) shows that BESS can provide/absorb power to/from LVDN even if the system mismatch power fluctuates drastically. It can be seen that the BESS power outputs can track the system power mismatch by using the proposed controller. Fig.7 (e) shows the results that SoC and proportions of BESS are gradually synchronized even if system power is changing. While the triggered events are showing in Fig.7 (e), where it can be observed that communication is reduced since there is a good deal of un-triggered events during the control process. Results from Fig.7 illustrated that the proposed power sharing controller (9) is capable to achieve SoC and proportion synchronization with reduced communication even if the system mismatch power and communication networks are all fluctuating.

4. Case Studies

This section validates the effectiveness of the proposed control and voltage regulation strategy of BESS. In simulations, a realistic low-voltage distribution network of southwest China, shown in Fig. 1, is built in MATLAB, where 9 PV stations and 9 BESSs with different parameters are installed in the distribution network. The resistance and reactance of the distribution lines are $0.35\Omega/km$ and $0.06\Omega/km$, respectively. The length of distribution line cables are also illustrated in Fig. 1.

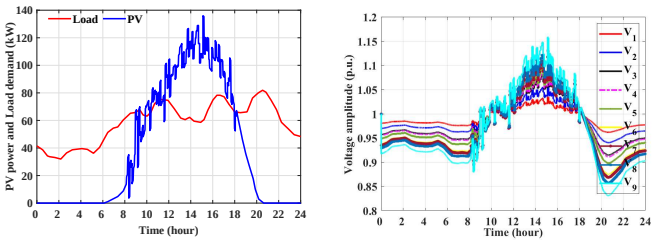

(a) (b)

Figure 8: The fluctuation of system power and voltages. (a) the PV power and load demand; (b) nodal voltage amplitudes.

Moreover, the parameters of BESS and PV stations are listed in Tab. 2 and Tab. 3. The PV active power output and load demand of the distribution network are shown in Fig. 8. From Fig.8, it can be seen that PV power varies from zero to 120 kW, meanwhile load demand is changing from 30 to 80 kW. During about 10:00 am to 6:00 pm, the total PV power output is larger than load demand, which in turn leads to the voltage-rise problem. When load demand is higher than PV power output, nodal voltages of some nodes are below the lower limit, shown in Fig8.

Table 2: Parameters of BESS

Sources	P^{max}	$P^{min}(kW)$	C_i	States
$BESS_1$	100	-100	100 (kWh)	SoC=60%
$BESS_2$	150	-150	150 (kWh)	SoC=58%
$BESS_3$	200	-200	200 (kWh)	SoC=62%
$BESS_4$	250	-250	250 (kWh)	SoC=66%
$BESS_5$	180	-180	180 (kWh)	SoC=56%
$BESS_6$	120	-120	120 (kWh)	SoC=54%
$BESS_7$	110	-110	110 (kWh)	SoC=52%
$BESS_8$	160	-160	160 (kWh)	SoC=68%
$BESS_9$	220	-220	220 (kWh)	SoC=70%

Table 3: Parameters of PV Stations

Sources	PV_1	PV_2	PV_3	PV_4	PV_5
$P^{max}(kW)$	12	24	9	15	18
$P^{min}(kW)$	0	0	0	0	0
Sources	PV_6	PV_7	PV_8	PV_9	
$P^{max}(kW)$	12	15	18	24	
$P^{min}(kW)$	0	0	0	0	

4.1. Performance with BESS: without energy and power sharing method

In this section, nine BESSs with different parameters are connected to the low-voltage DN. Each BESS adjusts the output power according to the controller (4) with $U_i(t) = 0$, $i = 1, \cdots, 9$. The PV power outputs and load demand are shown in Fig.8(a). The power outputs, SoC and system voltages are shown in Fig. 9, from which it can be seen that BESS power outputs are changing from -16 kW to 30 kW, meanwhile the SoC values are varying from 20% to 80%. This is because some of BESSs inject power to LVDN in order to drive nodal voltages above the lower limit, while other BESSs absorb power from gird to drive nodal voltages below the upper limit, which leads to the divergence of SoC values. From about 5:00 am to 10:00 am, SoC values of $BESS_{7,8,9}$ reach to the low limit. $BESS_{7,8,9}$ fail to inject power into LVDN to drive voltages back to the normal range. Thus, voltages of these nodes are below the lower voltage limit (0.95 p.u.). Power outputs and SoC values of $BESS_{1,2}$ maintain unchanged, since voltages at these nodes are always within the normal range.

4.2. Performance with BESS: Energy and power sharing method

In this section, BESS with energy and power sharing method is adopted to regulate system voltage, while PV power outputs and load demand are shown in Fig.8(a). The simulation results

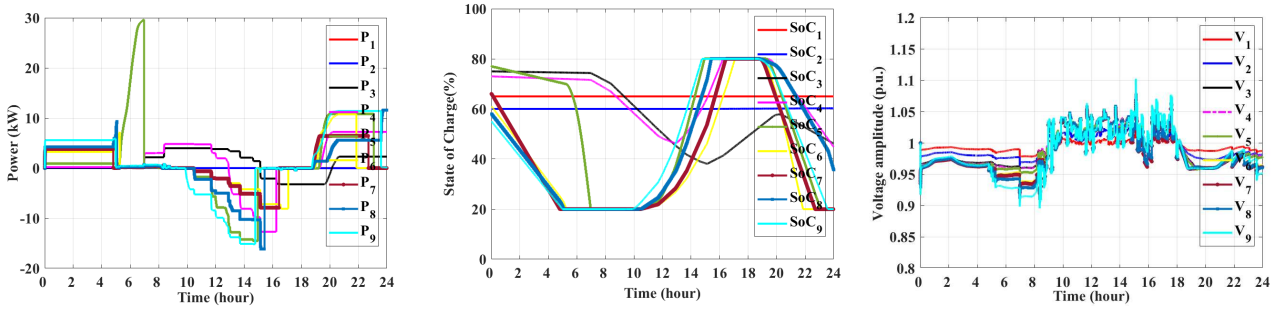

(a) (b) (c)

Figure 9: The fluctuation of BESS power and nodal voltages. (a) the PV power and load demand; (b) the SoC of BESS. (c) nodal voltage amplitudes with $\alpha_1 = \alpha_2 = 40$ (W/V).

are shown in Fig. 10 and Fig. 11. From Fig. 10, it can be seen that BESS power outputs are changing from -10 kW to 10 kW, proportions of BESS are changing from -0.04 to 0.035, and SoC values of BESS are varying from 25% to 75%. From Fig. 11(a), it can be seen that nodal voltages fluctuate in the normal range at most of time, except the time instants with the rapid PV power fluctuations. All BESSs participate in the voltage regulation cooperatively. Thanks to the designed control method (9), SoC values and proportions of BESS are converged even with the condition that BESS participates in the process of voltage regulation.

In addition, with the proposed event-triggered information delivery strategy, the states of BESS are transmitted over the communication network only when the trigger function satisfies. The triggered events are shown in Fig. 11(b), from which it is observed that communication times decrease.

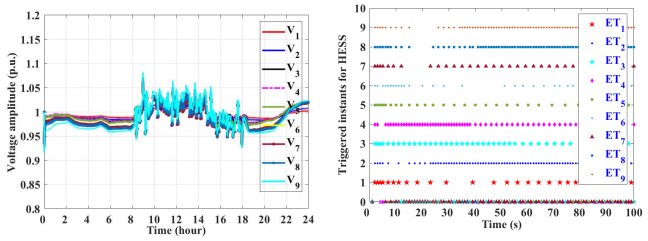

(a) (b)

Figure 11: (a) the fluctuation of system voltages; (b) the triggered events of BESS.

4.3. Performance with BESS and Time-varying Communication Networks

This section investigates the impact of time-varying communication networks on system performance. As shown in Fig. 12, the communication networks among distributed BESS are changing from G_1 to G_2, from G_2 to G_3 and from G_3 to G_1 periodically. The simulation results with the proposed control method are shown in Fig. 13. In Fig. 13(c), it can be seen that nodal voltages are varying in the normal range at most of time even though the communication links between BESSs are disconnected. Therefore, the proposed method is capable to

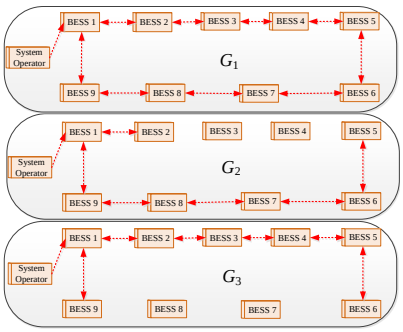

Figure 12: The time-varying communication networks.

adapt the time-varying networks with guaranteed performance as long as the feedback control gain is designed in term of (23). It can be observed in Fig. 13(a) and (b) that the power outputs, SoC values and proportions of BESS are gradually converging with the results obtained from the time-varying communication networks. However, it should be noted that the time-varying communication network should be continuously connected, which ensures that the local information could be shared globally.

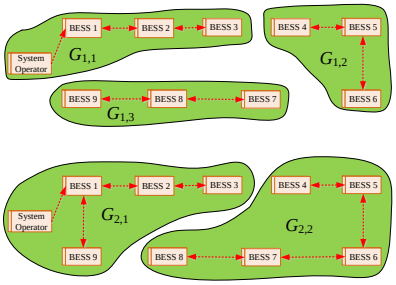

Figure 14: The original communication network is divided into several subgraphs.

4.4. Impacts of Communication Link Failures

As shown in Fig.14, the original communication network G_1 is divided into tree subgraphs $G_{1,1}$, $G_{1,2}$ and $G_{1,3}$ from $t = 0$:

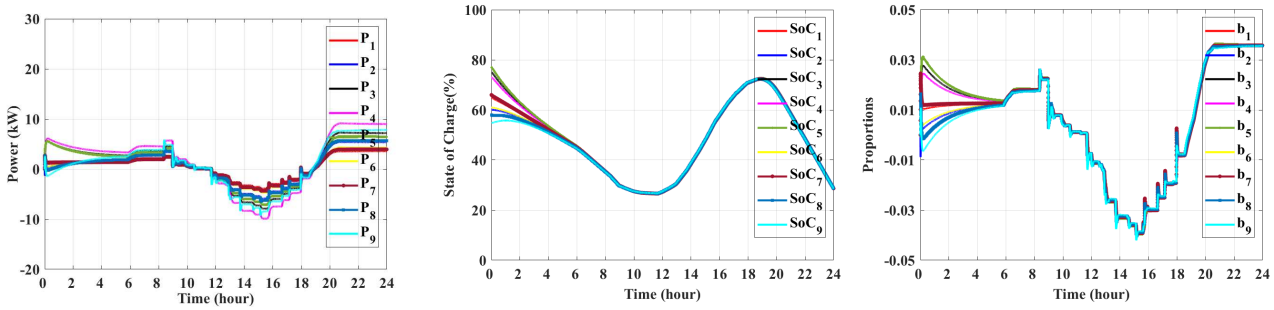

(a) (b) (c)

Figure 10: States of distributed BESS with time-invariant networks with $\kappa = [-20,\ 1.1]$ and parameter $\delta = 0.1$. (a) the power outputs of BESS; (b) SoC values of BESS; (c) the proportions of BESS.

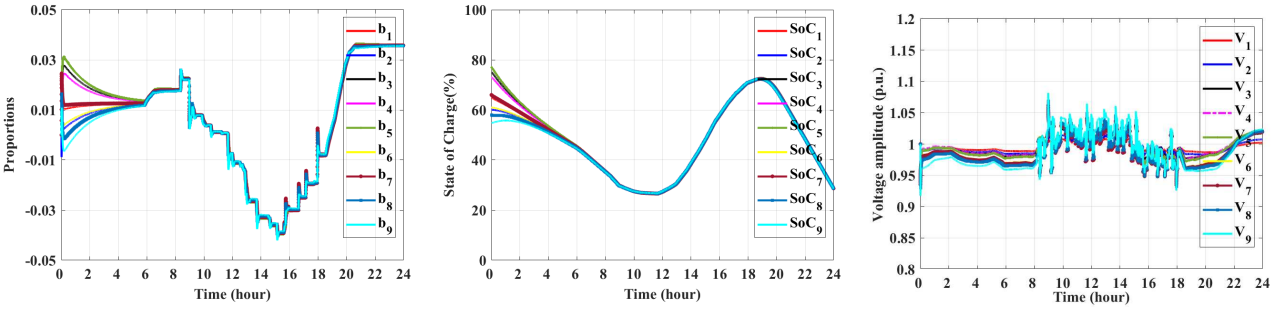

(a) (b) (c)

Figure 13: States of BESS over time-varying communication networks with $\kappa = [-20,\ 1.1]$ and parameter $\delta = 0.1$. (a) the proportions of BESS; (b) the SoC values of BESS; (c) nodal voltages.

00 to $t = 6:00$, and then divided into two subgraphs $G_{2,1}$ and $G_{2,2}$ from $t = 6:00$ to $t = 14:00$. After $14:00$, the communication network becomes to G_1. The simulation results are shown in Fig.15, from which it can be seen from $t = 0:00$ to $t = 6:00$, the proportions and SoC values of BESS in each subgraphs converge to the same value, however the average values of each subgraphs are different. From $t = 6:00$ to $t = 14:00$, the proportions and SoC values of $\text{BESS}_{1,2,3,9}$ and $\text{BESS}_{4,5,6,7,8}$ converge, respectively. After $t = 14:00$, proportions and SoC values of all BESS converge gradually, shown in Fig.15(a) and (b). However, the system voltages still vary in the normal range because BESS regulates voltage by using the local droop control.

4.5. Impacts of BESS Constraints

This section investigates the impacts of constraints of BESS on the voltage performance. Fig.16 (a) and (b) are the obtained results when the range of SoC is set as $[35\%, 70\%]$. It can be seen from Fig.16 (a) that during about $8:00$ to $12:00$ and $23:00$ to $24:00$ SoC of BESS reaches to the low bound (35%) due to the discharging, and during about $16:00$ to $21:00$, SoC of BESS reaches to the high bound (70%). When SoC reaches the low bound, BESS will not provide power to LVDN so that nodal voltages can not be driven into the normal range. On the contrary, BESS ceases to charge when SoC reaches its high bound which in turn leads nodal voltages to remain above the upper voltage limit. The impacts on voltage regulation are shown in Fig.16 (b).

Fig.16 (c) and (d) are the results when considering BESS power constraints. This case study investigates the voltage regulation performance when BESS power is constrained into a small range. It can be seen from Fig.16 (c) that BESS power outputs are all constrained into the range of $[-5, 5]$ (kW). Under this case study, fluctuation of nodal voltages is shown in Fig.16 (d). When nodal voltage is high than the upper voltage limit, BESS can not absorb surplus power from LVDN because of the power constraints. On the other hand, BESS also can to provide enough power to LVDN when nodal voltage is below the bottom voltage limit. This is verified by results in Fig.16 (d). Constraints of BESS SoC and power are important to achieve nodal voltage regulation in LVDN. Under the extreme situations when BESS can not provide/absorb active power to/from LVDN because of constraints, curtailing PV active power outputs is one possible way to achieve voltage regulation in LVDN.

5. Conclusion

In order to drive the system voltages of LVDN with high penetrated PV systems into the normal range, this paper proposed a distributed voltage regulation method with distributed heterogeneous BESS. It has been shown that system voltages are restored by proper power sharing among heterogeneous BESS. Besides, communication burdens are relieved largely by using

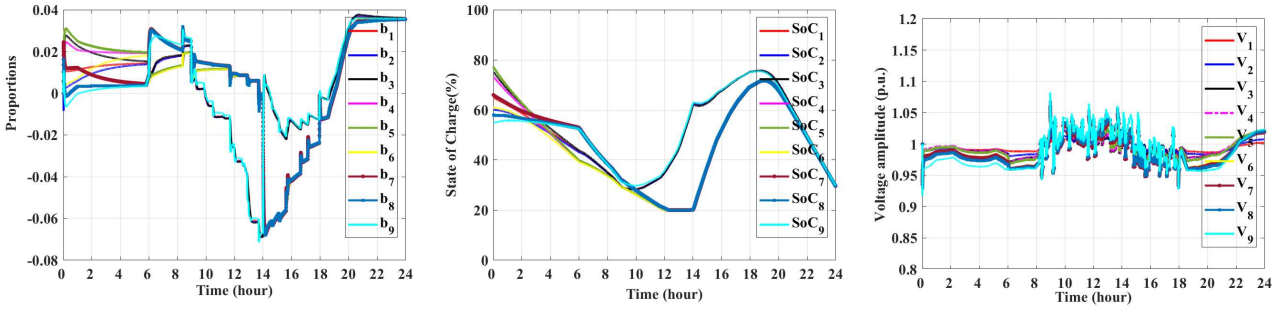

(a) (b) (c)

Figure 15: States of BESS with $\kappa = [-20,\ 1.1]$ and parameter $\delta = 0.1$. (a) the proportions of BESS; (b) the SoC values of BESS; (c) system voltages.

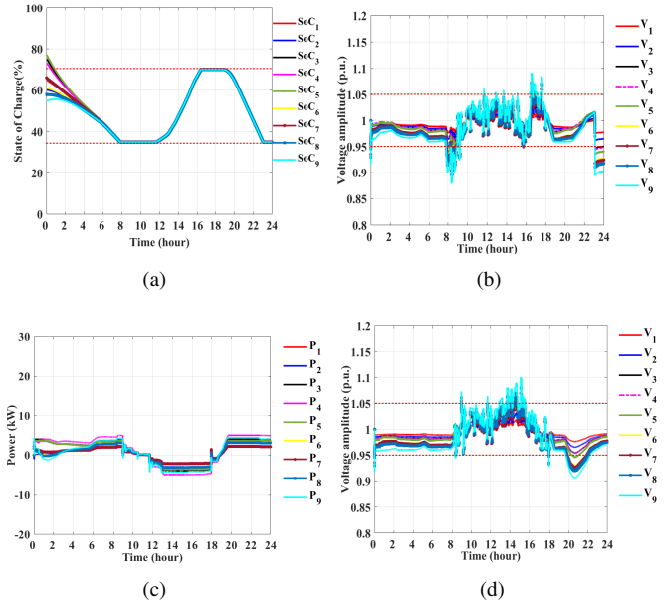

(a) (b) (c) (d)

Figure 16: Impacts of BESS constraints on voltage regulation. (a) the SoC values of BESS with constraints; (b) fluctuation of nodal voltages with SoC constraints; (c) power outputs of BESS with constraints; (d) fluctuation of nodal voltages with power constraints.

the dynamic event-triggered communication strategy. Even if the communication network among BESS changes, the proposed method also ensures a satisfied performance. Four simulation case studies based on LVDN of a real village from the south-west China are provided to validate the effectiveness of the proposed method. Studies show that for a LVDN with high-penetrated PV systems, nodal voltages could violate the upper/lower limits. With the adjustment of BESS power, which may be with different parameters, nodal voltages can be driven into the normal range in a short time. Future works may include investigating the effects of communication delays and cyber attacks on the communication networks.

Acknowledgments

This work was supported in part by the National "111" Project of China (under Grant No. B08036) and in part by the China Scholarship Council(No. CSC:201906050079). W. Baoze, J. C. Vasquez, and J. M. Guerrero were supported by VILLUM FONDEN under the VILLUM Investigator Grant (no. 25920): Center for Research on Microgrids (CROM); www.crom.et.aau.dk.

References

[1] B. Durlinger, A. Reinders, and M. Toxopeus, "Environmental benefits of pv powered lighting products for rural areas in south east asia: A life cycle analysis with geographic allocation," in *2010 35th IEEE Photovoltaic Specialists Conference*, 2010, pp. 002 353–002 357.

[2] T. Winarko, N. Hariyanto, F. S. Rahman, M. Watanabe, and Y. Mitani, "Cost-benefit analysis of pv penetration and its impact on the frequency stability: Case study of the south-central kalimantan system," in *2019 IEEE Innovative Smart Grid Technologies - Asia (ISGT Asia)*, 2019, pp. 1700–1705.

[3] M. S. Ali, M. M. Haque, and P. Wolfs, "A review of topological ordering based voltage rise mitigation methods for lv distribution networks with high levels of photovoltaic penetration," *Renewable and Sustainable Energy Reviews*, vol. 103, pp. 463 – 476, 2019. [Online]. Available: http://www.sciencedirect.com/science/article/pii/S1364032118308517

[4] K. Mahmoud and M. Lehtonen, "Comprehensive analytical expressions for assessing and maximizing technical benefits of photovoltaics to distribution systems," *IEEE Transactions on Smart Grid*, pp. 1–1, 2021.

[5] J. Viana, V. Palacios, M. Snchez, and J. Espinosa, "Multiarea secondary voltage regulation with optimal shunt elements coordinated maneuvers," in *2019 IEEE 4th Colombian Conference on Automatic Control (CCAC)*, 2019, pp. 1–6.

[6] G. Joksimovic, "Transformer voltage regulationan alternative expression," *IEEE Transactions on Power Delivery*, vol. 27, no. 2, pp. 1023–1024, 2012.

[7] V. S.-P. Cheung, H. S.-h. Chung, and A. W.-L. Lo, "A modular and scalable structure using multiparallel-connected series-voltage compensators for supply voltage regulation," *IEEE Transactions on Power Electronics*, vol. 31, no. 6, pp. 4096–4110, 2016.

[8] Y. Tan, C. Liao, Y. Li, Y. Cao, M. Shahidehpour, and C. Chen, "A linear power flow model for balanced distribution network with droop-controlled dstatcom and voltage controlled dg," *International Journal of Electrical Power & Energy Systems*, vol. 117, p. 105665, 2020. [Online]. Available: http://www.sciencedirect.com/science/article/pii/S0142061518328618

[9] S. Ghosh, S. Rahman, and M. Pipattanasomporn, "Distribution voltage regulation through active power curtailment with pv inverters and solar generation forecasts," *IEEE Transactions on Sustainable Energy*, vol. 8, no. 1, pp. 13–22, 2017.

[10] M. Zeraati, M. E. Hamedani Golshan, and J. M. Guerrero, "A consensus-based cooperative control of pev battery and pv active power curtailment for voltage regulation in distribution networks," *IEEE Transactions on Smart Grid*, vol. 10, no. 1, pp. 670–680, 2019.

[11] D. Cao, W. Hu, J. Zhao, Q. Huang, Z. Chen, and F. Blaabjerg, "A multi-agent deep reinforcement learning based voltage regulation using coordinated pv inverters," *IEEE Transactions on Power Systems*, vol. 35, no. 5, pp. 4120–4123, 2020.

[12] M. Al-Saffar and P. Musilek, "Reinforcement learning-based distributed bess management for mitigating overvoltage issues in systems with high pv penetration," *IEEE Transactions on Smart Grid*, vol. 11, no. 4, pp. 2980–2994, 2020.

[13] K. R. Reddy and S. Meikandasivam, "Load flattening and voltage regulation using plug-in electric vehicle's storage capacity with vehicle prioritization using anfis," *IEEE Transactions on Sustainable Energy*, vol. 11, no. 1, pp. 260–270, 2020.

[14] P. Yu, C. Wan, Y. Song, and Y. Jiang, "Distributed control of multi-energy storage systems for voltage regulation in distribution networks: A back-and-forth communication framework," *IEEE Transactions on Smart Grid*, vol. 12, no. 3, pp. 1964–1977, 2021.

[15] C. Feng, Z. Li, M. Shahidehpour, F. Wen, W. Liu, and X. Wang, "Decentralized short-term voltage control in active power distribution systems," *IEEE Transactions on Smart Grid*, vol. 9, no. 5, pp. 4566–4576, 2018.

[16] H. Ji, C. Wang, P. Li, J. Zhao, G. Song, F. Ding, and J. Wu, "A centralized-based method to determine the local voltage control strategies of distributed generator operation in active distribution networks," *Applied Energy*, vol. 228, pp. 2024–2036, 2018. [Online]. Available: https://www.sciencedirect.com/science/article/pii/S0306261918310936

[17] X. Hu, Z.-W. Liu, G. Wen, X. Yu, and C. Liu, "Voltage control for distribution networks via coordinated regulation of active and reactive power of dgs," *IEEE Transactions on Smart Grid*, vol. 11, no. 5, pp. 4017–4031, 2020.

[18] Y. Chai, L. Guo, C. Wang, Z. Zhao, X. Du, and J. Pan, "Network partition and voltage coordination control for distribution networks with high penetration of distributed pv units," *IEEE Transactions on Power Systems*, vol. 33, no. 3, pp. 3396–3407, 2018.

[19] P. Li, H. Ji, H. Yu, J. Zhao, C. Wang, G. Song, and J. Wu, "Combined decentralized and local voltage control strategy of soft open points in active distribution networks," *Applied Energy*, vol. 241, pp. 613–624, 2019. [Online]. Available: https://www.sciencedirect.com/science/article/pii/S0306261919304295

[20] Y. Guo, H. Gao, and Z. Wang, "Distributed online voltage control for wind farms using generalized fast dual ascent," *IEEE Transactions on Power Systems*, vol. 35, no. 6, pp. 4505–4517, 2020.

[21] W. Kang, M. Chen, W. Lai, and Y. Luo, "Distributed real-time power management of high-penetrated pv sources with voltage regulation over time-varying networks," *International Journal of Electrical Power & Energy Systems*, vol. 129, p. 106720, 2021. [Online]. Available: https://www.sciencedirect.com/science/article/pii/S0142061520342642

[22] W. Jiao, J. Chen, Q. Wu, S. Huang, C. Li, and B. Zhou, "Distributed coordinated voltage control for distribution networks with dg and oltc based on mpc and gradient projection," *IEEE Transactions on Power Systems*, pp. 1–1, 2021.

[23] Y. Wang, K. T. Tan, X. Y. Peng, and P. L. So, "Coordinated control of distributed energy-storage systems for voltage regulation in distribution networks," *IEEE Transactions on Power Delivery*, vol. 31, no. 3, pp. 1132–1141, 2016.

[24] X. Wang, C. Wang, T. Xu, L. Guo, P. Li, L. Yu, and H. Meng, "Optimal voltage regulation for distribution networks with multi-microgrids," *Applied Energy*, vol. 210, pp. 1027–1036, 2018. [Online]. Available: https://www.sciencedirect.com/science/article/pii/S0306261917311376

[25] M. Zeraati, M. E. Hamedani Golshan, and J. M. Guerrero, "Distributed control of battery energy storage systems for voltage regulation in distribution networks with high pv penetration," *IEEE Transactions on Smart Grid*, vol. 9, no. 4, pp. 3582–3593, 2018.

[26] M. Zeraati, M. E. H. Golshan, and J. M. Guerrero, "Voltage quality improvement in low voltage distribution networks using reactive power capability of single-phase pv inverters," *IEEE Transactions on Smart Grid*, vol. 10, no. 5, pp. 5057–5065, 2019.

[27] B. A. Faiya, D. Athanasiadis, M. Chen, S. McArthur, I. Kockar, H. Lu, and F. de Len, "A self organizing multi agent system for distributed voltage regulation," *IEEE Transactions on Smart Grid*, pp. 1–1, 2021.

[28] L. Xing, Y. Mishra, Y.-C. Tian, G. Ledwich, C. Wen, W. He, W. Du, and F. Qian, "Distributed voltage regulation for low-voltage and high-pv-penetration networks with battery energy storage systems subject to communication delay," *IEEE Transactions on Control Systems Technology*, pp. 1–8, 2021.

[29] W. Ma, W. Wang, Z. Chen, X. Wu, R. Hu, F. Tang, and W. Zhang, "Voltage regulation methods for active distribution networks considering the reactive power optimization of substations," *Applied Energy*, vol. 284, p. 116347, 2021. [Online]. Available: https://www.sciencedirect.com/science/article/pii/S0306261920317293

[30] Z. Zhang, F. F. da Silva, Y. Guo, C. L. Bak, and Z. Chen, "Double-layer stochastic model predictive voltage control in active distribution networks with high penetration of renewables," *Applied Energy*, vol. 302, p. 117530, 2021. [Online]. Available: https://www.sciencedirect.com/science/article/pii/S0306261921009090

[31] F. U. Nazir, B. C. Pal, and R. A. Jabr, "Distributed solution of stochastic volt/var control in radial networks," *IEEE Transactions on Smart Grid*, vol. 11, no. 6, pp. 5314–5324, 2020.

[32] B. A. Faiya, D. Athanasiadis, M. Chen, S. McArthur, I. Kockar, H. Lu, and F. de Len, "A self-organizing multi-agent system for distributed voltage regulation," *IEEE Transactions on Smart Grid*, vol. 12, no. 5, pp. 4102–4112, 2021.

[33] X. Wang, C. Wang, T. Xu, H. Meng, P. Li, and L. Yu, "Distributed voltage control for active distribution networks based on distribution phasor measurement units," *Applied Energy*, vol. 229, pp. 804–813, 2018. [Online]. Available: https://www.sciencedirect.com/science/article/pii/S0306261918311966

[34] G. Mokhtari, A. Ghosh, G. Nourbakhsh, and G. Ledwich, "Smart robust resources control in lv network to deal with voltage rise issue," *IEEE Transactions on Sustainable Energy*, vol. 4, no. 4, pp. 1043–1050, 2013.

[35] H. E. Z. Farag and E. F. El-Saadany, "A novel cooperative protocol for distributed voltage control in active distribution systems," *IEEE Transactions on Power Systems*, vol. 28, no. 2, pp. 1645–1656, 2013.

[36] M. Baran and F. Wu, "Network reconfiguration in distribution systems for loss reduction and load balancing," *IEEE Transactions on Power Delivery*, vol. 4, no. 2, pp. 1401–1407, 1989.

[37] J. Khazaei and Z. Miao, "Consensus control for energy storage systems," *IEEE Transactions on Smart Grid*, vol. 9, no. 4, pp. 3009–3017, July 2018.

[38] K. S. Ng, C.-S. Moo, Y.-P. Chen, and Y.-C. Hsieh, "Enhanced coulomb counting method for estimating state-of-charge and state-of-health of lithium-ion batteries," *Applied Energy*, vol. 86, no. 9, pp. 1506 – 1511, 2009. [Online]. Available: http://www.sciencedirect.com/science/article/pii/S0306261908003061

[39] X. Lu, K. Sun, J. M. Guerrero, J. C. Vasquez, and L. Huang, "State-of-charge balance using adaptive droop control for distributed energy storage systems in dc microgrid applications," *IEEE Transactions on Industrial Electronics*, vol. 61, no. 6, pp. 2804–2815, 2014.